

Characterization on AISI 316L Stainless Steel; Boriding, Nitriding and Boriding-Nitriding

Gerardo Pérez Mendoza¹, Noe Lopez Perrusquia¹, Marco Doñu Ruiz¹, Lizbeth Melo-Máximo² and Ismael Lopez Velazquez¹

¹Universidad Politecnica del Valle de México, Mexico, Distrito Federal, Mexico, ²Tecnológico de Monterrey, Mexico, Distrito Federal, Mexico,

The variety of surface treatment processes in 316L stainless steels permits the formation of hard surfaces, with the intention of improve its performance and to be used widely in the industry [1]; However there are few studies and evidence on results of hard surface formation, obtained by a mixture of dehydrated boron paste, salt nitriding and the combination of both processes [2-3]. This study shows the effect of surface treatments on 316L stainless steel.

The chemical composition of AISI 316L stainless steel is: 0.03% C, 2.0% Mg, 0.03% P, 0.03% S, 0.75% Si, 20% Cr, 14% Ni, 4% Mo. Three surface treatments applied on samples stainless steels: Boriding, Nitriding and Boriding-Nitriding. The boriding process was realized by dehydrated paste in box in a conventional furnace without inert gas, using a mixture of 70wt% reused boron and 30wt% pure boron at a temperature of 900°C for 2 h; next, it was removed out of the furnace to obtain the ambient temperature. The nitriding process was realized in a furnace for salts with of 50wt% Potassium Nitrate and 50wt% Sodium Nitrate at 550°C for 2 h, continuing with cooling in the salts to 350°C for 0.25 h reaching the ambient temperature out of the salt furnace. The Boriding-Nitriding duplex process was performed; first boriding and second nitriding with the times and temperatures established in this study.

The layers formed on the 316L stainless steel surface were then studied using a Scanning Electron Microscope JSM-IT100, to determine the morphology, layer structure and layer thickness. The layers obtained were analyzed by means of a Bruker D8 Advance Diffractometer with a radiation CuK α wavelength $\lambda=1.54$ A at a speed of 2°/min.

Figure 1a) shows the formation the boride layers, exhibited a monolayer structure flat Fe₂B whit thickness of 5.89 μ m; the EDS analysis shown the presence of B, Cr, N,C. Figure 1b) shows the formation nitride layers, revealed a layer structure flat Fe₃N and Fe₃N with a thickness of 3.51 μ m and EDS analysis shown the presence of Mn, Cr, Ni on layer nitride, Figure 1c) shows the formation the layer by boriding-nitriding, exhibited a multilayer structure flat with a thickness of 26.07 μ m. In addition, a crack is evident in the mixture layer caused by tension and compression stresses from the Boriding-Nitriding process and EDS analysis reveals a high concentration of Oxygen, and also the presence of N,B,Mn,Cr.

Figure 2a) The XRD analysis confirmed the presence of the Fe₂B phase and CrB, Ni₃B for the boriding process by combination dehydrated boron paste. For Figure 2b) XRD analysis confirmed the presence of a layer formed by the phases CrN, Fe₄N, Fe₃N and CrO₃by salt nitriding process. Figure 2c) XRD analysis reveals in the mixture layer, the presence of Fe₄N and B_xN, phases obtained by the boriding-nitriding process. In addition is revealed Fe₂O₃, FeBO₃ and Cr₂O₃ oxides, caused by the in the salt nitriding process. The boron paste dehydrated mixture shows an effect for the formation of the boride layer. The Salts nitriding produces a combined nitride layer. The combined boriding-nitriding treatment has an influence on the growth and thickness of the multilayer.

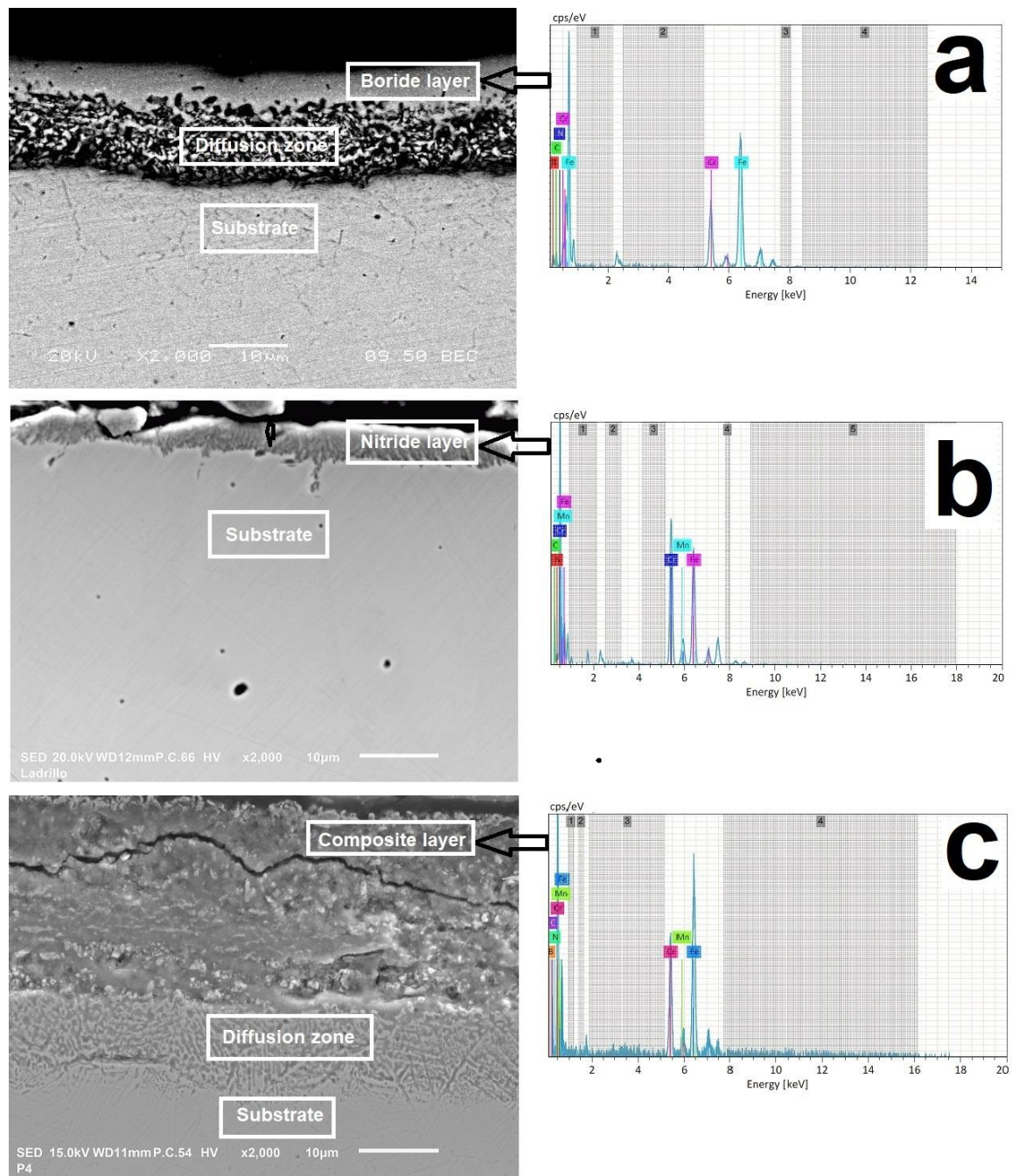


Figure 1. SEM micrograph shows the AISI 316L stainless steel; (a) Layer of Boride at 900°C by 2 h, (b) Layer of Nitride of 550°C by 2 h and (c) Layer of Boriding-Nitriding

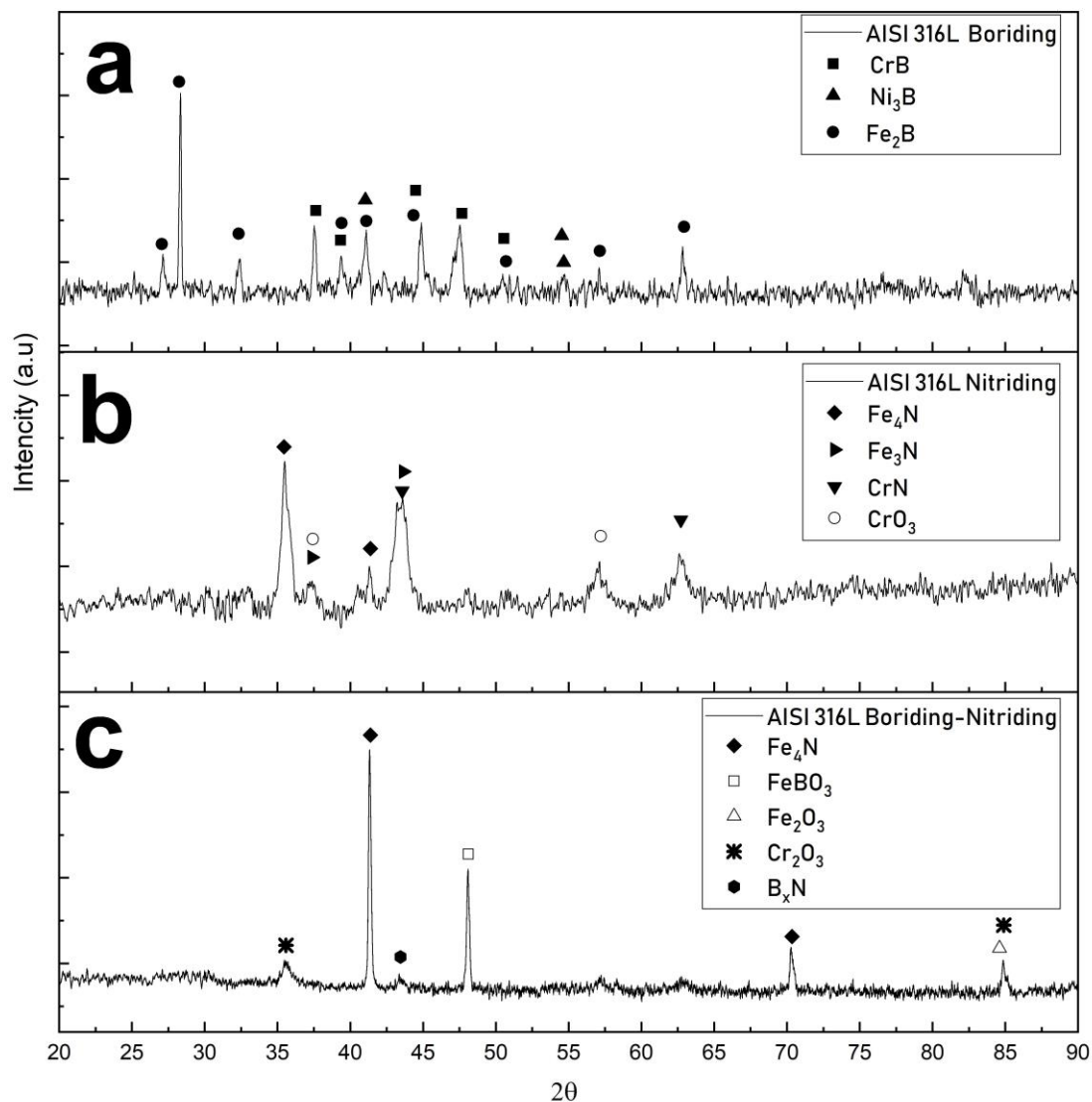


Figure 2. XRD diffraction patterns obtained on surface of AISI 316L stainless steel; (a) Boriding by dehydrated paste, (b) Nitriding in salts and (c) Boriding-Nitriding

References

- [1] I. E. Campos-Silva and G.A. Rodríguez-Castro, Thermochemical Surface Engineering of Steels, 1st ed., E.J. Mittemeijer and M.A.J. Somers, Ed., Woodhead-Elsevier Publishing, Cambridge, 2015, p. 651–697.
- [2] G. Pérez Mendoza et. al., Microscopy and Microanalysis. **25(S2)** (2019), p. 2398-2399
- [3] O. A. Gómez-Vargas et. al., Microscopy and Microanalysis. **25(S2)** (2019), p. 796-797